JACS
JOURNAL OF THE AMERICAN CHEMICAL SOCIETY

Article

pubs.acs.org/JACS

Efficient Conversion of CO_2 to CO Using Tin and Other Inexpensive and Easily Prepared Post-Transition Metal Catalysts

Jonnathan Medina-Ramos, Rachel C. Pupillo, Thomas P. Keane, John L. DiMeglio, and Joel Rosenthal*

Department of Chemistry and Biochemistry, University of Delaware, Newark, Delaware 19716, United States

Supporting Information

ABSTRACT: The development of affordable electrocatalysts that can drive the reduction of CO_2 to CO with high selectivity, efficiency, and large current densities is a critical step on the path to production of liquid carbon-based fuels. In this work, we show that inexpensive triflate salts of Sn^{2+}, Pb^{2+}, Bi^{3+}, and Sb^{3+} can be used as precursors for the electrodeposition of CO_2 reduction cathode materials from MeCN solutions, providing a general and facile electrodeposition strategy, which streamlines catalyst synthesis. The ability of these four platforms to drive the formation of CO from CO_2 in the presence of [BMIM]OTf was probed. The electrochemically prepared Sn and Bi catalysts proved to be highly active, selective, and robust platforms for CO evolution, with partial current densities of j_{CO} = 5−8 mA/cm^2 at applied overpotentials of η < 250 mV. By contrast, the electrodeposited Pb and Sb catalysts do not promote rapid CO generation with the same level of selectivity. The Pb material is only ∼10% as active as the Sn and Bi systems at an applied potential of E = −1.95 V and is rapidly passivated during catalysis. The Sb-comprised cathode material shows no activity for conversion of CO_2 to CO under analogous conditions. When taken together, this work demonstrates that 1,3-dialkylimidazoliums can promote CO production, but only when used in combination with an appropriately chosen electrocatalyst material. More broadly, these results suggest that the interactions between CO_2, the imidazolium promoter, and the cathode surface are all critical to the observed catalysis.

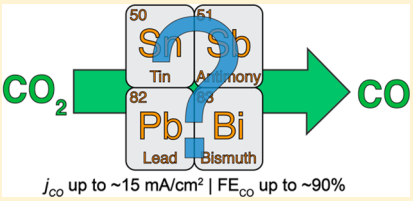

INTRODUCTION

The generation of CO via the $2e^-/2H^+$ reduction of CO_2 is a reaction of fundamental importance to the field of molecular energy conversion.[1,2] This electrochemical half reaction produces an energy rich commodity chemical that is a key starting material for the synthesis of methanol,[3−5] as well as organic acids,[6−8] aldehydes,[9] and alcohols.[10] Moreover, carbon monoxide is the critical C_1 feedstock for Fischer−Tropsch (FT)[11−13] and electrolytic methods[14,15] that deliver synthetic petroleum, hydrocarbons, and oxygenates. As such, the efficient production of CO from nonpetroleum resources is a critical step toward the sustainable production of liquid fuels.[16] One promising strategy to accomplish this goal is the marriage of renewable sources of electric energy with cathode materials that are robust and can promote the conversion of CO_2 to CO with high selectivity (i.e., Faradaic efficiency (FE_{CO})) and activity (i.e., partial current density (j_{CO})) at low applied overpotentials (η).

Several cathode materials are known to catalyze the conversion of CO_2 to CO;[17,18] however, until recently, only precious metals such as Ag[19−21] and Au[22−24] could promote this process with Faradaic Efficiencies (FEs) above 80% while displaying high current density (competent rate) at modest overpotentials.[25] Because the exorbitant price of these precious metals is incompatible with schemes to produce renewable fuels on a commercial scale, the search for new inexpensive materials that drive CO evolution with reasonable activity at low overpotential is a critical step on the path to the sustainable production of carbon-based fuels from renewable energy sources.

Although most inexpensive metallic cathodes typically require very large overpotentials in order to activate CO_2,[26] our laboratory recently demonstrated that an economical bismuth-based material could promote the electrochemical conversion of CO_2 to CO with high efficiency and selectivity.[27] This bismuth−carbon monoxide evolving catalyst (Bi-CMEC) was prepared using a straightforward electrodeposition method to produce a robust Bi^0/Bi^{III} containing material on conducting carbon substrates from strongly acidic aqueous solutions containing low concentrations of Bi^{3+} salts.

Efficient CO production was realized with this Bi-modified carbon electrode in CO_2 saturated MeCN containing millimolar concentrations of a 1,3-dialkyl substituted imidazolium based ionic liquid (IL) promoter such as 1-butyl-3-methylimidazolium triflate ([BMIM]OTf).[27] Under these conditions, the Bi-CMEC/IL system was found to drive CO production with high selectivity (FE_{CO} > 80%) and impressive kinetics (j_{CO} = 5−25 mA/cm^2) at an applied cathode potential of −1.95 to −2.0 V versus SCE. As has been observed for other heterogeneous[28−30] and homogeneous[31] systems for CO_2 electrocatalysis, the presence of the imidazolium IL promoter in the electrolyte solution significantly improves the activity for CO evolution using Bi-CMEC. The promotion effect was

Received: December 8, 2014
Published: February 19, 2015

DOI: 10.1021/ja5121088
J. Am. Chem. Soc. 2015, 137, 5021−5027

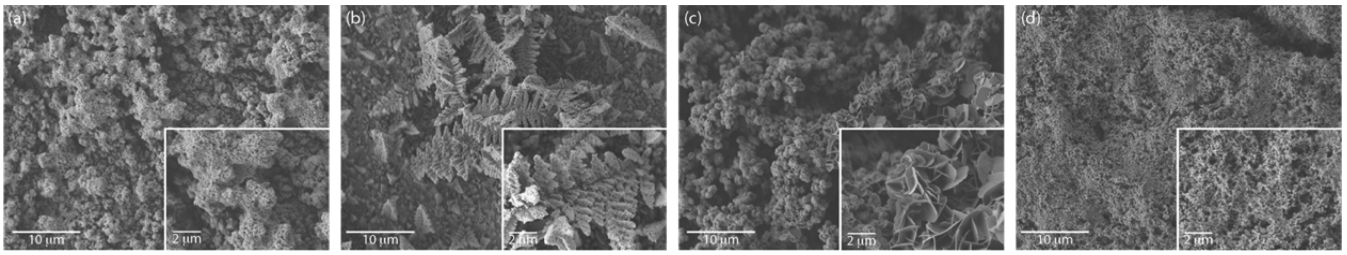

Figure 1. SEM images of electrodeposited cathode materials derived from (a) $Bi(OTf)_3$, (b) $Sn(OTf)_2$, (c) $Pb(OTf)_2$, and (d) $Sb(OTf)_3$.

observed using $[BMIM]^+$ ILs comprised of a number of common anions including OTf^-, PF_6^-, BF_4^-, and halides.[32]

In addition to being able to form Bi-CMEC modified electrodes from acidic aqueous solutions, this catalyst platform can also be prepared via in situ electrodeposition methods from MeCN/$[BMIM]^+$ electrolyte solutions that contain low concentrations of $Bi(OTf)_3$.[32] The ability to electrodeposit Bi-CMEC from noncaustic organic solutions streamlines preparation and study of the material while enabling the use of conducting supports that normally would not tolerate the strongly acidic media required for aqueous electrodeposition. Building on this previous work, we wondered whether bismuth, as well as tin and other inexpensive post-transition metals could be prepared ex-situ from an organic catholyte and promote CO evolution using the same MeCN/$[BMIM]^+$ electrolyte system that had been successfully employed with the Bi-CMEC platform. We were also curious to see if the imidazolium additive would ensure efficient CO_2 activation irrespective of the post-transition metal cathode material employed or if cathode materials other than bismuth would display distinct activities and reactivity profiles for CO_2 reduction.

RESULTS AND DISCUSSION

Thin film materials based upon bismuth, tin, lead, and antimony were prepared using a facile electrodeposition method. Polarization of an inert glassy carbon or nickel working electrode at potentials between −1.25 and −1.55 V versus SCE (all potentials are reported with respect to this reference) in an MeCN solution containing 0.1 M $TBAPF_6$ and 20 mM of either $Bi(OTf)_3$, $Sn(OTf)_2$, $Pb(OTf)_2$, or $Sb(OTf)_3$ led to electrodeposition of dark-colored films onto the inert electrode substrate. Thin films for each of the above p-block metal triflate salts were electrodeposited to a total thickness of 1.0 C/cm^2 and were analyzed by a combination of physical methods.

The morphology of each of the electrodeposited materials was probed by scanning electron microscopy (SEM), as shown in Figure 1. The electrodeposited Bi based material is visualized as an amorphous granular material (Figure 1a), which bears some resemblance to the electrochemically prepared Sb-based deposits (Figure 1d). The other two electrodeposited materials have a unique appearance under magnification. The Sn-based electrodeposits appear as micrometer sized crystallites that bear resemblance to the fronds of a fern, whereas the electrodeposited Pb material is visualized as an array of striated clusters.

The elemental composition of each of the materials of Figure 1 was analyzed using energy-dispersive X-ray (EDX) spectroscopy. EDX analysis was performed on 40 × 40 μm^2 regions of multiple independently prepared samples of each post-transition metal modified electrode (Supporting Information Figure S1). This analysis revealed that each electrodeposited material contained the respective post-transition metal along with oxygen, fluorine, and phosphorus (presumably from the $CF_3SO_3^-$ and PF_6^- in the electrodeposition baths). The surface of each material was also analyzed by X-ray photoelectron spectroscopy (XPS), which identified O, F, and the corresponding post-transition metal as the principal elemental components of the deposited materials, along with trace amounts of S, N, and P from $CF_3SO_3^-$, Bu_4N^+, and PF_6^- ions that were incorporated into the electrodeposited films (Supporting Information Figures S2−S5).

Closer inspection of XPS spectra for the Bi, Sn, Pb, and Sb regions of the four different modified electrodes showed that the major post-transition metal component for each material does not exist in the metallic state (Figure 2). For example, the

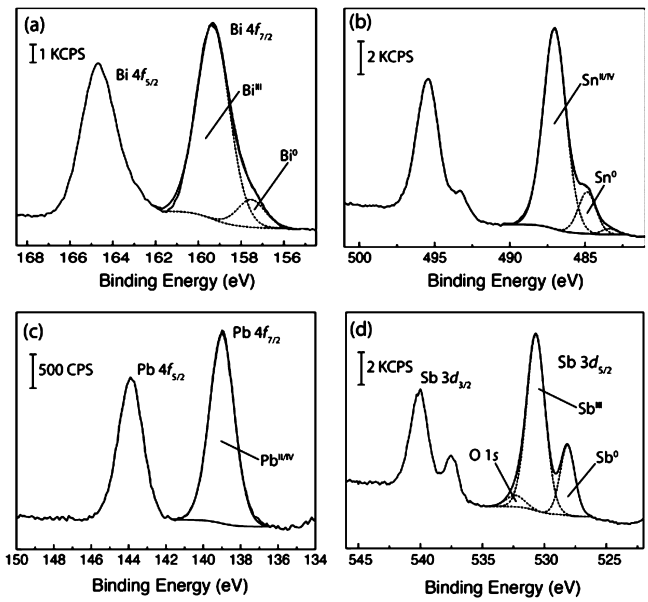

Figure 2. High-resolution XPS spectra recorded for (a) Bi $4f_{7/2}$ region of the Bi-modified electrode, (b) Sn $3d_{5/2}$ region of the Sn-modified electrode, (c) Pb $4f_{7/2}$ region of the Pb-modified electrode, and (d) Sb $3d_{5/2}$ region of the Sb-modified electrode.

high-resolution Bi $4f_{7/2}$ spectrum recorded for the Bi-modified electrode was fitted to two components at 159.4 and 157.6 eV that correspond to Bi^{3+} and Bi^0, respectively.[33] The ratio of these two components was 94:6, indicating that that the overwhelming majority of the surface of the electrodeposited Bi-material exists in an oxidized state (Supporting Information Figure S2). A similar situation was observed for the other three materials surveyed. The respective high-resolution XPS spectra recorded for the Sn-modified electrode showed two peaks in the Sn $3d_{5/2}$ region at 487.0 and 484.9 eV (Supporting

DOI: 10.1021/ja5121088
J. Am. Chem. Soc. 2015, 137, 5021−5027

Information Figure S3), which correspond to $Sn^{2+/4+}$ and Sn^0 in a ratio of 86:14.[33] This composition is similar to that observed to electrodeposited Sn/SnO_x films prepared from aqueous solutions.[34]

High-resolution XPS spectra recorded for the Sb-modified electrode showed two peaks in the Sb $3d_{5/2}$ region at 530.5 and 528.1 eV (Supporting Information Figure S4), which correspond to Sb^{3+} and Sb^0 in a ratio of 81:19.[33] Lastly, high-resolution XPS spectra recorded for the Pb-modified electrode showed only a single peak in the Pb $4f_{7/2}$ region at 139.0 eV (Supporting Information Figure S5), which corresponds to $Pb^{2+/4+}$.[33] XPS did not show any evidence for metallic lead on the surface of the electrodeposited Pb material. When taken together, the EDX and XPS analyses indicate that the surface of the post-transition metal materials shown in Figure 1 that are electrodeposited from solutions of the appropriate $M(OTf)_n$ salts in MeCN containing $TBAPF_6$ contain little to none of the metallic (M^0) p-block element. Instead the modified electrodes are coated in films that are largely comprised of M^{n+} ions that have incorporated a significant amount of oxygen and fluoride to balance the charge of the metal ions.

The ability of each of the electrodeposited materials to electrochemically activate CO_2 was assessed in MeCN containing 100 mM [BMIM]OTf. This solvent/IL combination supports a large electrochemical window and was previously employed for CO_2 conversion studies involving Bi-CMEC.[27,32] As shown in Figure 3, linear sweep voltammograms (LSVs) recorded in CO_2 saturated MeCN containing 100 mM [BMIM]OTf using glassy carbon or nickel electrodes modified with the four materials described above, results in polarization curves with onset potentials that vary from approximately −1.8 to −1.95 V.

Of the four electrodeposited films, the Bi-based material shows the earliest onset potential of ∼ −1.8 V, followed by Sn and Sb at approximately −1.85 V and Pb at −1.95 V. LSVs recorded under the same conditions but in the absence of CO_2 do not show any appreciable rise in current (Supporting Information Figures S6−S9). This observation is consistent with the large current responses shown in Figure 3 being due to CO_2 activation/conversion at each of the modified cathode assemblies.

Although the ability of Bi-CMEC to drive the electrocatalytic conversion of CO_2 to CO has been demonstrated, the effect that oxygen and fluorine incorporation into the Bi-based cathode material might have on the ability of this platform to promote CO_2 conversion was not clear. Moreover, the ability of Sn and Sb-based materials to promote the electrochemical reduction of CO_2 to CO in MeCN/IL electrolytes had not been previously ascertained. In order to establish that the electrochemical responses shown for the cathode materials of Figure 1 correspond to conversion of CO_2 to CO, controlled potential electrolysis (CPE) experiments were carried out for CO_2 saturated solutions of MeCN containing 100 mM [BMIM]OTf. Given the fact that both the electrodeposited Bi and Sn materials showed similar onset potentials in the presence of the IL promoter at approximately −1.8 V, we initially probed the ability of these two cathode materials to promote CO_2 reduction at −1.95 V. Since these electrochemical experiments were conducted under conditions of low proton availability, the equilibrium potential ($E^\circ_{CO_2/CO}$) for conversion of CO_2 to CO under the MeCN/$[BMIM]^+$ catholyte conditions employed in this study can be computed

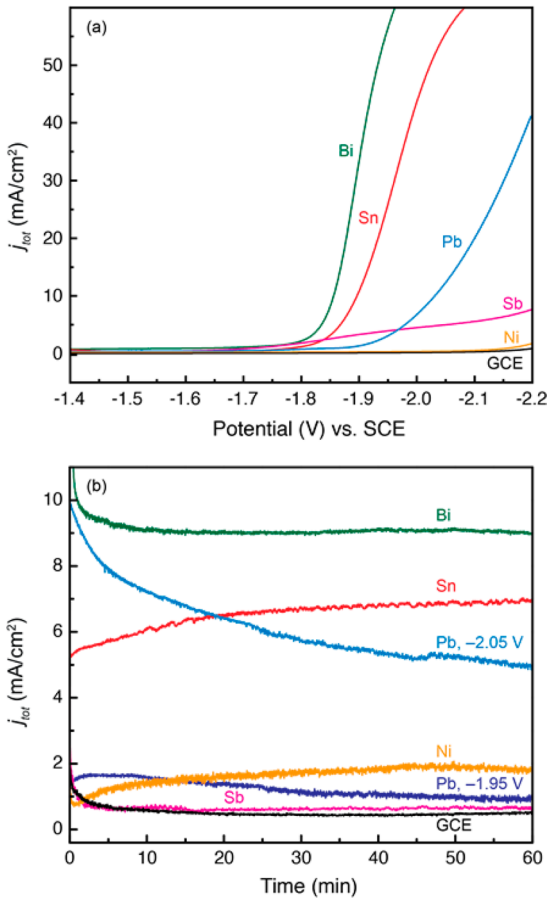

Figure 3. (a) Linear sweep voltammograms (LSVs) and (b) total current density profiles recorded for electrodeposited cathode materials in CO_2 saturated MeCN containing 100 mM [BMIM]OTf. Current density plots for which no potential is listed were recorded at −1.95 V versus SCE.

as is described in the Supporting Information[35] and previous studies.[27,32,36] We note that the value of $E^\circ_{CO_2/CO}$ under the conditions employed in this study, is within 100 mV of the catalytic onset potentials observed for CO_2 reduction by the Bi- and Sn-based materials.

Upon initiating CPE experiments at −1.95 V for electrodes modified with the Bi, Sn, Pb, or Sb materials described above, the reaction headspace was periodically analyzed by gas chromatography. This analysis showed that for the Bi- and Sn-modified electrodes, CO was the only gaseous product formed during the electrolysis experiment, with no detected coproduction of H_2, CH_4, or other small hydrocarbons. Quantification of the gas produced showed that polarization of the Bi and Sn materials at −1.95 V leads to the evolution of CO with FEs of 78% and 77%, respectively. Under these CPE conditions, these materials were found to promote the $2e^-/2H^+$ conversion of CO_2 to CO with appreciable partial current densities that were measured to be $j_{CO} = 8.4 \pm 1.7$ mA/cm^2 for Bi and $j_{CO} = 5.0 \pm 1.8$ mA/cm^2 for Sn (Table 1).

Analysis of the catholyte solutions at the end of the CPE experiments by NMR spectroscopy showed coproduction of a small amount of formate (FE ∼5%) using the Sn-modified electrode, however, no oxalate or glyoxalate was detected. Nonvolatile CO_2 reduction products were not observed in the catholyte solutions following CPE experiments that employed the Bi-modified electrodes. That these carboxylate containing

DOI: 10.1021/ja5121088
J. Am. Chem. Soc. 2015, 137, 5021−5027

Table 1. Faradaic Efficiencies (FE) and Current Densities (j) for Electrocatalytic reduction of CO_2 in MeCN containing 100 mM [BMIM]OTf

electrode	E_{appl} (η)	j_{tot} (mA/cm^2)	FE_{CO}	FE_{H_2}	FE_{HCO_2H}	j_{co} (mA/cm^2)
Bi	−1.95 V (~200 mV)	10.1 ± 2.1	78 ± 5%			8.4 ± 1.7
Sn	−1.95 V (~200 mV)	7.2 ± 1.9	77 ± 5%		5 ± 1%	5.0 ± 1.8
Sb	−1.95 V (~200 mV)	0.5 ± 0.1		30 ± 20%	29 ± 21%	
Pb	−1.95 V (~200 mV)	1.0 ± 0.4	40 ± 12%	11 ± 6%	31 ± 17%	0.4 ± 0.2
Pb	−2.05 V (~300 mV)	5.0 ± 1.0	81 ± 5%			4.1 ± 0.9

products are not formed to any significant extent using the Bi- and Sn-modified electrodes is noteworthy, as these species are often the dominant products observed upon reduction of CO_2 in organic catholytes.[37,38] Moreover, although formic acid is often the major product obtained upon reduction of CO_2 with cathodes based upon Bi[39] or Sn,[40−44] formation of this competing $2e^-/2H^+$ CO_2 reduction side product is overwhelmingly suppressed upon CPE of CO_2 using the electrodeposited Bi and Sn materials in MeCN/$[BMIM]^+$ catholyte solutions (Table 1).

When considering the product distribution outlined for the Bi and Sn materials in Table 1, roughly 20% of the charge passed during the CPE experiments is unaccounted for. This disparity may be due to formation of nonvolatile CO_2 reduction products at levels that are below our detection limits. For example, recent work has demonstrated that copper electrodes can promote the conversion of CO_2 to a slew of highly reduced C_2 and C_3 products, such as glycoaldehyde, acetaldehyde, acetate, and propionaldehyde, among others.[45] For the case of copper, and possibly for the cathode materials described here, each of these products are formed with current efficiencies below 1%. However, because formation of such highly reduced compounds requires the consumption of anywhere from 6 to 20 electron equivalents, a modest fraction of the overall catalytic current may be diverted to drive the formation of negligible amounts of C_2 or C_3 products. Additional unaccounted charge may be coopted to drive reduction of the oxidized Bi and Sn materials during the CPE experiments to generate catalyst films with greater proportions of the post-transition metal elements in the metallic state under in situ conditions.

Repetition of the above CPE experiments under an atmosphere of N_2 leads to negligible current densities for both the Bi and Sn materials (Supporting Information Figures S6 and S7). Further, CO was not formed under these conditions, indicating that the product obtained under CO_2 is not derived from the electrochemical decomposition of the $[BMIM]^+$ electrolyte. Similarly, repeating the above CPE experiments under an atmosphere of CO_2 but while using a more conventional organic electrolyte such as $TBAPF_6$ in place of [BMIM]OTf, results in little charge being passed and an overwhelming decrease in the FE for CO production (Supporting Information Figures S6−S7, Table S1). When taken together, these experiments establish that the imidazolium ($[BMIM]^+$) is critical to the observed electrocatalysis and promotes the selective production of CO from CO_2 with competent kinetics at both Bi- and Sn-based cathodes.

Upon establishing that the Bi- and Sn-modified electrodes could promote the rapid conversion of CO_2 to CO in the presence of [BMIM]OTf, we moved to ascertain how the Sb and Pb electrodeposited materials would compare. Repetition of the CPE experiment described above at −1.95 V using the Sb-modified electrode did not generate CO and resulted in very little charge being passed over the course of a 1 h experiment (Figure 3b, Table 1). The poor activity of the electrodeposited Sb material for CO_2 reduction is also reflected by the LSV recorded for this material under the CPE conditions (Figure 3a), which displays a level of current enhancement that is only slightly higher than that observed for the inert Ni and GCE substrates. Moreover, the current response obtained with the Sb-modified electrode is not significantly attenuated in the absence of CO_2 (Supporting Information Figure S8).

CPE experiments employing the Pb modified electrode resulted in a distribution of products that was dramatically different from those observed for Bi and Sn under the same conditions, with FEs for CO, H_2, and HCO_2H of 40%, 11%, and 31%, respectively (Table 1). In addition to the fragmented product distribution, under these CPE conditions, Pb operates with appreciably slower kinetics for CO evolution as compared to the Bi and Sn catalyst systems. Displaying a measured partial current density for CO production at −1.95 V of j_{CO} ~0.4 mA/cm^2, the Pb catalyst is less than 10% as active as Sn and 5% as active as the Bi homologue (Table 1). The lower activity of Pb is also reflected by the later onset potential for CO_2 reduction displayed by this cathode material, as compared to the Bi and Sn systems.

Although the Pb-modified electrode displays poor selectivity and kinetics for CO generation at −1.95 V, the general shape of the LSV recorded for this catalyst in the presence of CO_2 and [BMIM]OTf suggested that this system might display a more pronounced CO_2 conversion efficiency at higher applied overpotentials (Figure 2). When the CPE experiment described above is repeated with a Pb-modified electrode at an applied potential of −2.05 V, the selectivity of CO production is markedly improved as the recorded FE for this product is above 80% at these more negative potentials (Table 1). As expected, the kinetics of CO evolution at the Pb catalyst are also enhanced at −2.05 V to j_{CO} = 4.1 ± 0.9 mA/cm^2. Although it is not readily apparent why the selectivity for CO production at the Pb-cathode is markedly improved as the applied overpotential increases, one potential explanation for this behavior is that formic acid and CO are formed at Pb via distinct mechanistic pathways with differing Tafel profiles.[46] We note that many cathodes for CO_2 reduction display varied and complex product distribution profiles as a function of applied potential.[26] As was the case for the Bi- and Sn-modified electrodes, no current enhancement was observed for the Pb material in the absence of CO_2 or $[BMIM]^+$ (Supporting Information Figures S9).

In addition to displaying competent kinetics for CO evolution, the electrodeposited Pb material is also highly selective, as no coproduction of oxalate, glyoxalate or formate was detected in the catholyte following the CPE experiment at −2.05 V. The potential at which the electrodeposited Pb material evolves CO at a current density of 4−5 mA/cm^2 is more positive than that required to effect the same process

DOI: 10.1021/ja5121088
J. Am. Chem. Soc. 2015, 137, 5021−5027

using a piece of lead foil under similar CPE conditions by ~300 mV.[47] The improved performance of the electrodeposited Pb catalyst may originate from the porous surface structure of the material (Figure 1c), as compared to the flatter mesoscopic structure of more uniform bulk Pb substrates.

NMR analysis of the catholyte solutions following prolonged CPEs using either the Bi- or Sn-modified electrodes (at −1.95 V) or the Pb-modified assembly (at −2.05 V) did not reveal significant levels of $[BMIM]^+$ decomposition or formation of the imidazolium−carboxylate adduct $[BMIM{-}CO_2]$. Previous work has shown that such imidazolium−carboxylate adducts can be formed upon polarization of platinum[48] or lead foil electrodes[47] in the presence of [BMIM] and CO_2 at very negative potentials. The observation of rapid and selective conversion of CO_2 to CO with the Bi-, Sn-, and Pb-modified electrodes that we describe herein suggests that formation of $[BMIM{-}CO_2]$ and related species may occur via a pathway that is distinct from the electrolytic process that results in CO evolution. As such, the electrodeposited Bi, Sn, and Pb catalyst materials that are described above offer distinct advantages over other cathode/$[BMIM]^+$ systems because the electrodeposited materials can activate CO_2 at lower potentials, which circumvents the formation of imidazolium−carboxylate side products.

The CPE experiments described above demonstrate that the electrodeposited Bi, Sn, and Pb materials can all promote rapid conversion of CO_2 to CO with good selectivity at low overpotential when in the presence of [BMIM]OTf. However, the Pb material is not as robust during the CPE as compared to the other two post-transition metal materials. As shown in Figure 3, over the course of a 60 min CPE experiment at −2.05 V, the current density obtained with a Pb-based cathode is not steady, and slowly decays below 4−5 mA/cm^2. This drop in the rate of CO production continues upon prolonged electrolysis and is accompanied by a dramatic decrease in the FE of CO generation, which plateaus at ~10% (Supporting Information Figure S10). These observations suggest that the electrodeposited Pb material either degrades or becomes passivated during catalysis. The same loss in activity is not observed for the electrodeposited Bi and Sn materials for which stable current densities and FEs for CO evolution are maintained for at least 6−8 h (Supporting Information Figure S10), suggesting that these latter two materials are neither passivated nor degraded during electrocatalysis.

Of the four electrodeposited materials, only the Bi- and Sn-based cathodes proved to be robust, selective, and kinetically competent catalysts for the cathodic half reaction that generates CO. We thus turned our attention to optimizing these two platforms. Increasing the concentration of [BMIM]OTf in the catholyte solution leads to an enhanced current response. The current response corresponding to CO_2 reduction plateaus at a $[BMIM]^+$ concentration of ~300 mM for both the electrodeposited Bi and Sn materials. CPE experiments were conducted at −1.95 V using these cathode materials suspended in CO_2 saturated MeCN containing 300 mM [BMIM]OTf. Under these conditions, the Bi-modified electrode displays impressive enhancements in selectivity and activity, with partial current density for CO production of j_{CO} = 14 ± 2 mA/cm^2 and FE_{CO} = 80%. An even more striking improvement in CO evolution activity and catalytic efficiency is realized for the Sn-modified electrode, which operated with a partial current density of j_{CO} = 13 ± 3 mA/cm^2 and FE_{CO} = 91%. These metrics are extremely noteworthy, as they demonstrate that the Sn-modified electrode can catalyze the conversion of CO_2 to CO with a level of efficiency and selectivity that is typically only accessible with precious metal catalysts that are both rare and expensive. *As such, the Sn-modified electrode described herein is, to the best of our knowledge, the only example to date of a heterogeneous electrocatalyst platform consisting only of inexpensive and earth abundant elements that can efficiently promote the production of CO from CO_2 with current densities above 10 mA/cm^2 at low overpotentials.*

Repetition of the above CPE experiments under an atmosphere of N_2 lead to little passed charge and no CO production. Accordingly, it is highly unlikely that the improved selectivity and kinetics for CO generation realized upon use of higher $[BMIM]^+$ concentrations is due to imidazolium decomposition. Moreover, the metrics observed for conversion of CO_2 to CO using the electrodeposited Sn material are much better than those obtained using other tin-based systems, which typically promote the reduction of CO_2 to formate and additional products other than CO. Because the Sn-modified electrode is intimately involved in the electrocatalytic conversion of CO_2 to CO and promotes half-reaction with excellent current densities at low overpotentials, this system represents a Sn-carbon monoxide evolving catalyst (Sn-CMEC).

Because Sn-CMEC is a proficient system for CO_2 reduction, we pursued the in situ formation of this platform from the CO_2 saturated MeCN/$[BMIM]^+$ electrolyte, as has been done previously for Bi-CMEC. Such in situ electrodeposition strategies not only can streamline preparation of the catalyst material but also can allow for catalyst electrodeposition on substrates that are too delicate or reactive to survive excessive manipulation. Because the $Sn(OTf)_2$ salt is soluble in CO_2 saturated MeCN containing [BMIM]OTf and is reduced at a potential that is more positive than the onset potential for CO_2 reduction using Sn-CMEC, we suspected that this system would be a fine candidate for in situ catalyst electrodeposition.

Electrochemical reduction of CO_2 saturated solutions of MeCN containing 1.0 mM $Sn(OTf)_2$ and 100 mM [BMIM]-OTf show that this system promotes electrocatalysis. Cyclic voltammograms recorded for the above solution show a cathodic feature at appoximately E = −1.5 V, which corresponds to reduction of $Sn(OTf)_2$. This initial redox event is followed by an intense catalytic wave at E = −1.85 V (Figure 4a). This sharp current enhancement is nearly identical to the polarization curve recorded for CO_2 reduction using the ex-situ-generated Sn-CMEC (Figure 2a). This result suggests that cathodic polarization of the MeCN/[BMIM]OTf solution containing $Sn(OTf)_2$ leads to electrodeposition of a Sn-based material that can activate CO_2 at potentials that are more negative than −1.8 V. CV experiments conducted for MeCN solutions containing 1.0 mM $Sn(OTf)_2$ and 100 mM [BMIM]OTf but under an atmosphere of N_2 are consistent with this analysis; under these conditions (i.e., in the absence of CO_2), virtually no current enhancement is observed from −1.8 to −2.2 V. Similarly, CVs recorded in the absence of [BMIM]OTf show no current enhancement at these negative potentials indicating that Sn, $[BMIM]^+$, and CO_2 are all integral to the observed catalysis.

CPE experiments also demonstrate that the in situ generated Sn material is active for the conversion of CO_2 to CO. As shown by the green trace in Figure 4b, electrolysis of a CO_2 saturated solution of MeCN containing 100 mM [BMIM]OTf at −1.95 V using a Ni working electrodes exhibited low current

DOI: 10.1021/ja5121088
J. Am. Chem. Soc. 2015, 137, 5021−5027

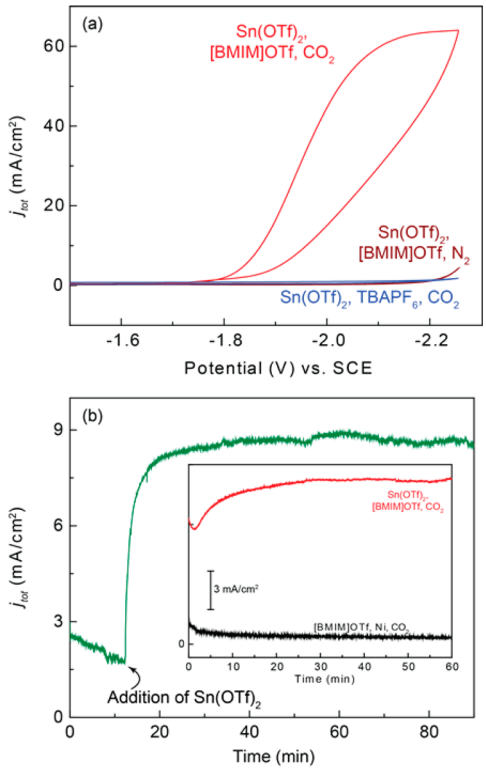

Figure 4. (a) CV traces recorded at a Ni disk electrode in MeCN solutions containing 1.0 mM $Sn(OTf)_2$ under an atmosphere of either CO_2 or N_2. (b) Total current density trace recorded for a Ni disk electrode at −1.95 V in MeCN containing 100 mM [BMIM]OTf before an after addition of 1 mM $Sn(OTf)_2$. Inset: partial current density profiles for CO production (j_{CO}) at a Ni disk electrode in MeCN containing 100 mM [BMIM]OTf in the presence (red) and absence (black) of 1.0 mM $Sn(OTf)_2$.

densities of $j_{tot} \sim 1.5$ mA/cm^2. No CO was detected under these conditions. Addition of $Sn(OTf)_2$ to the CPE solution led to a dramatic rise in current, which ultimately plateaued at $j_{tot} \sim 9$ mA/cm^2. This rise in current was accompanied by the formation of a dark film on the Ni cathode and the formation of CO as judged by periodic GC analysis of the reaction headspace. As was the case for the ex situ Sn-CMEC experiments, CO is the only gaseous product formed during the CPE. Quantification of the CO generated revealed that the in situ generated Sn-CMEC operates with $FE_{CO} \sim 75\%$ and an average partial current density of $j_{CO} = 9.8 \pm 2$ mA/cm^2. Repetition of this CPE experiment under N_2 leads to little passed charge and does not generate CO. Similarly, repeating this CPE experiment under CO_2 but in the absence of $Sn(OTf)_2$ leads to low current densities (~0.6 mA/cm^2) and virtually no CO production. These results are consistent with in situ generation of the Sn-CMEC catalyst and represent a promising strategy toward formation of a CO_2 reduction electrocatalyst that can be easily formed in situ from an inexpensive and earth abundant metal precursor and that operates with competent kinetics and efficiency.

■ CONCLUSIONS AND FUTURE DIRECTIONS

The efficient and rapid electrocatalytic conversion of CO_2 to CO using robust and inexpensive catalyst materials is a key milestone toward the storage of renewable energy and sustainable production of liquid fuels. Although cathodes based upon silver and gold can efficiently promote this chemistry, the demand for and scarcity of these materials has limited their use on the scale required for commercial fuel production. By contrast, tin, bismuth, lead, and other post-transition metals are significantly more affordable and are in some cases earth abundant. As such, the development of CO evolving catalyst platforms that utilize these elements is of great potential interest for electrochemical fuel production.

In the present study, we have shown that triflate salts of Sn^{2+}, Pb^{2+}, Bi^{3+}, and Sb^{3+} are excellent precursors for the electrodeposition of post-transition-metal-based cathode materials from organic electrolyte solutions. In the presence of a 1,3-dialkyl substituted imidazolium based IL, such as [BMIM]OTf, these platforms show varied activities and efficiencies for the electrolytic conversion of CO_2 to CO. Both the Sn- and Bi-based cathodes selectively catalyze the reduction of CO_2 to CO with partial current densities that range from approximately 5−10 mA/cm^2 under the MeCN/$[BMIM]^+$ electrolyte conditions employed for these studies. Moreover, both the Bi- and Sn-based electrocatalysts are robust and selectively promote CO evolution for at least 6−8 h. These metrics compare favorably to those obtained using precious metal CO_2 reduction cathodes and distinguish the electrodeposited Sn and Bi-containing materials detailed in this work as proficient carbon monoxide evolving catalysts (CMECs).

In contrast to the electrodeposited Sn-CMEC and Bi-CMEC platforms, similarly prepared materials derived from $Pb(OTf)_2$ or $Sb(OTf)_3$ in MeCN do not catalyze CO evolution with the same level of activity. Although the Sn- and Bi-based materials drive CO evolution at an applied potential of $E = -1.95$ V, the electrodeposited Pb material is less than 10% as active as these catalysts at the same applied potential. The electrodeposited Pb material can selectively promote CO evolution when polarized at more negative potentials but is rapidly passivated during catalysis, which limits the utility of this platform for electrolytic CO evolution. Although also easily prepared, the Sb-modified electrodes described in this work are not competent platforms for CO_2 conversion.

The facility with which the cathode materials detailed here have been prepared using a combination of ex situ and in situ electrodeposition methods, suggests that other inexpensive and easily prepared cathode materials may also be quickly prepared and screened for CO_2 reduction activity using an analogous approach. Extension of the $M(OTf)_n$ reduction strategy highlighted in this work to additional transition and main group metals triflates may streamline the preparation of new electrodeposited materials comprised of one or multiple metallic elements.

Although it is clear that the $[BMIM]^+$ component of these catalyst systems plays a pivotal role in promoting the efficient activation and reduction of CO_2 at the electrodeposited Sn-CMEC and Bi-CMEC platforms, utilization of this imidazolium with an arbitrarily chosen cathode material does not guarantee an efficient electrocatalysis with CO_2. For example, CPE of CO_2 saturated solutions of MeCN containing 300 mM [BMIM]OTf at −1.95 V using inert GCE or nickel foil electrodes does not result in an appreciable current response or the formation of CO_2 reduction products (Supporting Information Table S1). Similarly, CPEs conducted using an Sb-modified glassy carbon electrode do not generate CO and result in very little charge being passed over the course of a 1 h experiment (Table 1). Because the electrolytic reduction of CO_2 in the presence of imidazolium-based promoters is sensitive to the identity of the cathode material, it is clear

DOI: 10.1021/ja5121088
J. Am. Chem. Soc. 2015, 137, 5021−5027

that the observed CO evolution electrocatalysis that we observe cannot simply be attributed to homogeneous reduction of the $[BMIM]^+$ or CO_2 in solution. Instead, the results we have presented suggest that the intimate interaction of either CO_2, imidazolium, or both with the polarized Bi-CMEC and Sn-CMEC architectures is critical to the catalysis observed for these systems. Future work from our lab will be aimed at probing the nature of these complex interactions in an effort to optimize existing and innovate new CO_2 reduction platforms.

■ ASSOCIATED CONTENT

Supporting Information

High-resolution XPS spectra, control electrochemistry experiments, and experimental details can be found in the Supporting Information section. This material is available free of charge via the Internet at http://pubs.acs.org.

■ AUTHOR INFORMATION

Corresponding Author

joelr@udel.edu

Notes

The authors declare no competing financial interest.

■ ACKNOWLEDGMENTS

The efforts of J.L.D. to conduct electrode dynamics measurements were supported by Fluid Interface Reactions, Structures and Transport (FIRST) Center, an Energy Frontier Research Center funded by the U.S. Department of Energy, Office of Science, Office of Basic Energy Sciences. We thank Prof. Thomas P. Beebe for providing access to the XPS spectrometer used in this study and Tian Qiu for assistance in the preparation of lead and antimony triflate salts. J.R. was supported through a DuPont Young Professor Award. Additional financial support for this work was provided by the University of Delaware.

■ REFERENCES

(1) Benson, E. E.; Kubiak, C. P.; Sathrum, A. J.; Smieja, J. M. *Chem. Soc. Rev.* **2008**, *38*, 89−99.

(2) Whipple, D. T.; Kenis, P. J. A. *J. Phys. Chem. Lett.* **2010**, *1*, 3451−3458.

(3) Lee, S. *Methanol Synthesis Technology*; CRC Press: Boca Raton, Fl, 1989.

(4) Klier, K. *Adv. Catal.* **1982**, *31*, 243−313.

(5) Burch, R.; Golunski, S. E.; Spencer, M. S. *Faraday Trans.* **1990**, *86*, 2683−2691.

(6) Singh, A. D.; Krase, N. W. *Ind. Eng. Chem.* **1935**, *27*, 909−914.

(7) Jones, J. H. *Platinum Metals Rev.* **2000**, *44*, 94−105.

(8) Cheung, H.; Tanke, R. S.; Torrence, G. P. Acetic Acid. In *Ullmann's Encyclopedia of Industrial Chemistry*; Wiley-VCH: Weinheim, Germany, 2000.

(9) Ojima, I.; Tsai, C.-Y.; Tzamarioudaki, M.; Bonafoux, D. *Org. React.* **2000**, *56*, 1.

(10) Henrici-Olivé, G.; Olivé, S. Springer-Verlag: Berlin, 1984.

(11) Rofer-DePoorter, C. K. *Chem. Rev.* **1981**, 447−474.

(12) Vennestrøm, P. N. R.; Osmundsen, C. M.; Christensen, C. H.; Taarning, E. *Angew. Chem., Int. Ed.* **2011**, *50*, 10502−10509.

(13) Takeshita, T.; Yamaji, K. *Energy Policy* **2008**, *36*, 2773−2784.

(14) Li, C. W.; Ciston, J.; Kanan, M. W. *Nature* **2014**, *508*, 504−507.

(15) Gattrell, M.; Gupta, N.; Co, A. *J. Electroanal. Chem.* **2006**, *594*, 1−19.

(16) Rosenthal, J. *Prog. Inorg. Chem.* **2014**, *59*, 299−338.

(17) Azuma, M.; Hashimoto, K.; Hiramoto, M.; Watanabe, M.; Sakata, T. *J. Electrochem. Soc.* **1990**, *137*, 1772−1778.

(18) Hori, Y.; Kikuchi, K.; Suzuki, S. *Chem. Lett.* **1985**, *14*, 1695−1698.

(19) Hoshi, N.; Kato, M.; Hori, Y. *J. Electroanal. Chem.* **1997**, *440*, 283−286.

(20) Salehi-Khojin, A.; Jhong, H.-R. M.; Rosen, B. A.; Zhu, W.; Ma, S.; Kenis, P. J. A.; Masel, R. I. *J. Phys. Chem. C* **2013**, *117*, 1627−1632.

(21) Tornow, C. E.; Thorson, M. R.; Ma, S.; Gewirth, A. A.; Kenis, P. J. A. *J. Am. Chem. Soc.* **2012**, *134*, 19520−19523.

(22) Hori, Y.; Murata, A.; Kikuchi, K.; Suzuki, S. *J. Chem. Soc., Chem. Commun.* **1987**, *10*, 728−729.

(23) Chen, Y.; Li, C. W.; Kanan, M. W. *J. Am. Chem. Soc.* **2012**, *134*, 19969−19972.

(24) Zhu, W.; Michalsky, R.; Metin, Ö.; Lv, H.; Guo, S.; Wright, C. J.; Sun, X.; Peterson, A.; Sun, S. *J. Am. Chem. Soc.* **2013**, *135*, 16833−16836.

(25) Hori, Y.; Wakebe, H.; Tsukamoto, T.; Koga, O. *Electrochim. Acta* **1994**, *39*, 1833−1839.

(26) Hori, Y. *Mod. Aspects Electrochem.* **2008**, *42*, 89−189.

(27) DiMeglio, J. L.; Rosenthal, J. *J. Am. Chem. Soc.* **2013**, *135*, 8798−8801.

(28) Rosen, B. A.; Salehi-Khojin, A.; Thorson, M. R.; Zhu, W.; Whipple, D. T.; Kenis, P. J. A.; Masel, R. I. *Science* **2011**, *334*, 643−644.

(29) Rosen, B. A.; Haan, J. L.; Mukherjee, P.; Braunschweig, B.; Zhu, W.; Salehi-Khojin, A.; Dlott, D. D.; Masel, R. I. *J. Phys. Chem. C* **2012**, *116*, 15307−15312.

(30) Rosen, B. A.; Zhu, W.; Kaul, G.; Salehi-Khojin, A.; Masel, R. I. *J. Electrochem. Soc.* **2012**, *160*, H138−H141.

(31) Grills, D. C.; Matsubara, Y.; Kuwahara, Y.; Golisz, S. R.; Kurtz, D. A.; Mello, B. A. *J. Phys. Chem. Lett.* **2014**, *5*, 2033−2038.

(32) Medina-Ramos, J.; DiMeglio, J. L.; Rosenthal, J. *J. Am. Chem. Soc.* **2014**, *136*, 8361−8367.

(33) *Handbook of Photoelectron Spectroscopy*; Chastain, J., King, R. C., Jr., Eds.; Physical Electronics: Eden Prairie, MN, 1995.

(34) Chen, Y.; Kanan, M. W. *J. Am. Chem. Soc.* **2012**, *134*, 1986−1989.

(35) Determination of $E°CO_2/CO$ in [BMIM]+/MeCN electrolyte is presented in the Supporting Information.

(36) Costentin, C.; Drouet, S.; Robert, M.; Savéant, J. M. *Science* **2012**, *338*, 90−94.

(37) Ikeda, S.; Takagi, T.; Ito, K. *Bull. Chem. Soc. Jpn.* **1987**, *60*, 2517−2522.

(38) Amatore, C.; Savéant, J. M. *J. Am. Chem. Soc.* **1981**, *103*, 5021−5023.

(39) Komatsu, S.; Yanagihara, T.; Hiraga, Y.; Tanaka, M.; Kunugi, A. *Denki Kagaku* **1995**, *63*, 217−224.

(40) Köleli, F.; Atilan, T.; Palamut, N.; Gizir, A. M.; Aydin, R.; Hamann, C. H. *J. Appl. Electrochem.* **2003**, *33*, 447−450.

(41) Whipple, D. T.; Finke, E. C.; Kenis, P. J. A. *Solid-State Lett.* **2010**, *13*, B109−B111.

(42) Agarwal, A. S.; Zhai, Y.; Hill, D.; Sridhar, N. *ChemSusChem* **2011**, *4*, 1301−1310.

(43) Oloman, C.; Li, H. *ChemSusChem* **2008**, *1*, 385−391.

(44) Zhang, S.; Kang, P.; Meyer, T. J. *J. Am. Chem. Soc.* **2014**, *136*, 1734−1737.

(45) Kuhl, K. P.; Cave, E. R.; Abram, D. N.; Jaramillo, T. F. *Energy Environ. Sci.* **2012**, *5*, 7050−7059.

(46) Gileadi, E. *Electrode Kinetics for Chemists, Chemical Engineers and Materials Scientists*; Wiley-VCH: Weinheim, Germany, 1993.

(47) Sun, L.; Ramesha, G. K.; Kamat, P. V.; Brennecke, J. F. *Langmuir* **2014**, *30*, 6302−6308.

(48) de Robillard, G.; Devillers, C. H.; Kunz, D.; Cattey, H.; Digard, E.; Andrieu, J. *Org. Lett.* **2013**, *15*, 4410−4413.

DOI: 10.1021/ja5121088
J. Am. Chem. Soc. 2015, 137, 5021−5027